ELSEVIER

Earth and Planetary Science Letters 178 (2000) 303–314

EPSL

www.elsevier.com/locate/epsl

The effect of pressure on D_{Sr} (plag/melt) and D_{Cr} (opx/melt): implications for anorthosite petrogenesis

Jacqueline Vander Auwera [a,*], John Longhi [b], Jean Clair Duchesne [a]

[a] *L.A. Géologie, Pétrologie, Géochimie, Université de Liège, 4000 Liege, Belgium*
[b] *Lamont–Doherty Earth Observatory, Palisades, NY 10964, USA*

Received 2 February 1999; accepted 8 March 2000

Abstract

The crystal–liquid partition coefficients for Sr and Cr, D_{Sr} and D_{Cr}, have been determined from electron microprobe analyses of plagioclase–liquid and orthopyroxene–liquid pairs produced in melting experiments run at pressures from 1 bar to 27 kbar on two compositions relevant to anorthosite petrogenesis. One is a primitive jotunite (hypersthene monzodiorite: TJ); the other is a sample of an anorthositic dyke (500B). Results indicate that D_{Sr} (plag/liq) remains nearly constant with increasing pressure (TJ: 1.7 to 2.6; 500B: 0.9 to 1.4). This modest variation apparently results from the combined and opposing effects of crystal chemistry and pressure: D_{Sr} increases with the albite content of plagioclase, which itself increases with pressure along a composition's liquidus, so pressure must have an intrinsic negative effect. The two models for D_{Sr} [J. Blundy, B. Wood, Geochim. Cosmochim. Acta 55 (1991) 193–209; I. Bindeman, A. Davis, M. Drake, Geochim. Cosmochim. Acta 62 (1998) 1175–1193] that take into account the strong correlation between D_{Sr} and plagioclase composition overestimate D_{Sr} at high pressure; whereas the two models that ignore plagioclase composition [S. Morse, Geochim. Cosmochim. Acta 56 (1992) 1735–1738; R. Nielsen, Comput. Geosci. 18 (1992) 773–788] underestimate it. Moreover, since none of these models takes into account any pressure effect, the discrepancies between predicted and observed D_{Sr} increase with pressure for all models. The new results also show that D_{Cr} (opx/liq) increases significantly with pressure: $D_{Cr} = 2$ at 1 atm and 14.2 at 10 kbar. These new data confirm earlier, less precise determinations of D_{Cr} that were used to infer a high-pressure origin for Al- and Cr-rich orthopyroxene megacrysts. The calculated Sr and Cr concentrations of liquids in equilibrium at 10 kbar with plagioclase and orthopyroxene megacrysts from anorthosite massifs (Sr = 370 to 610 ppm and Cr = 20 to 130 ppm) are in the range of what is observed in high-Al gabbros and primitive jotunites, the inferred parent magmas of massive anorthosites.

Keywords: partition coefficients; plagioclase; orthopyroxene; anorthosite; continental crust

1. Introduction

The occurrence of plagioclase with intermediate composition (An_{35}–An_{65}) and high-Al orthopyroxene megacrysts is a well-known feature of many Proterozoic massive anorthosites [9–12]. Recent experimental data [2,8] indicate that the

* Corresponding author. Tel: +32-4-366-2253; E-mail: jvdauwera@ulg.ac.be

0012-821X/00/$ – see front matter
PII: S0012-821X(00)00086-8

intermediate composition of plagioclase as well as the high Al_2O_3 content of opx megacrysts are consistent with cotectic crystallization of broadly basaltic magmas at high pressures. On the other hand, petrological studies of contact aureoles of massive anorthosites (i.e. [1,13–15]) demonstrate that their final emplacement took place in the middle to upper crust. These two lines of evidence are the basis of polybaric petrogenetic models for massive anorthosites.

Plagioclase megacrysts from massive anorthosites are significantly richer in Sr than plagioclases from layered basic intrusions such as the Stillwater and Bushveld Complexes and an increase in the crystal–liquid partition coefficient for Sr between plagioclase and liquid (D_{Sr} (plag/liq)) with pressure might explain the differences [11]. Orthopyroxene megacrysts not only have high Al_2O_3 concentrations but also display unexpectedly high Cr contents [10,12] which are in apparent contradiction with their moderate Mg# ($\sim$0.75) and the intermediate Mg# ($\sim$0.5) of their inferred parent magma. Here too, an increase in the crystal–liquid partition coefficient for Cr between orthopyroxene and liquid (D_{Cr} (opx/melt)) with pressure appears plausible. In order to test possible pressure effects, we have determined D_{Sr} and D_{Cr} from electron microprobe analyses of plagioclase–liquid and orthopyroxene–liquid pairs produced in melting experiments on compositions relevant to anorthosite petrogenesis from 1 bar to 27 kbar. We have then used the high pressure (10 kbar) partition coefficients to estimate the Sr and Cr concentrations of liquids in equilibrium with plagioclase and orthopyroxene megacrysts from various occurrences and have compared them with the compositions of possible parent magmas.

2. Materials and methods

Melting experiments have been conducted on two powdered rocks (Table 1): the first, TJ, is a primitive jotunite (hypersthene monzodiorite) from Rogaland in Norway [1,16–17] and the second, 500B, is from an anorthositic dyke of the Nain Complex in Labrador [2–3]. Most of the experiments had been performed at Lamont–Doherty for previous studies [1–2] and several lines of observation in the experiments selected here (melt proportion above 80%, homogeneous liquid composition, Fe–Mg exchange partition coefficient between low-Ca pyroxene and melt in agreement with published values) suggest that equilibrium was approached [1]. The two starting compositions are quite different (Table 1): the normative composition of TJ is richer in mafic components ($\Sigma = 38.8\%$) than 500B ($\Sigma = 13.6\%$), whereas TJ is much lower in feldspathic components ($\Sigma = 59.9\%$) than 500B ($\Sigma = 83.8\%$).

Table 1
Composition of starting materials (wt% and CIPW norm)

	TJ	500B
SiO_2	49.39	55.85
TiO_2	3.67	0.52
Al_2O_3	15.81	22.92
FeO	10.60	3.26
Fe_2O_3[a]	2.79	0.27
MnO	0.13	0.06
MgO	4.54	1.40
CaO	6.87	9.55
Na_2O	3.50	4.67
K_2O	0.96	0.90
P_2O_5	0.71	0.16
Total	99.17	99.52
Qtz	1.75	2.46
Or	5.67	5.32
Ab	29.62	39.52
An	24.60	38.92
Di	4.01	6.21
Hy	20.66	5.39
Mgt	4.05	0.39
Il	6.97	0.99
Ap	1.64	0.37
Plag	An_{45}	An_{50}

[a]FeO and Fe_2O_3 contents were calculated at FMQ, 4 kbar and 1160°C for TJ and 1350°C for 500B [40].

Experiments were run in a standard 1/2 inch piston cylinder apparatus at high pressure and in a Deltech vertical furnace at 1 atm. Detailed experimental procedures are presented elsewhere [1–2]. As the purpose of this study is to assess the effect of pressure on D_{Sr} (plag/melt) and D_{Cr} (opx/melt), we selected two sets of liquidus or near liquidus experiments in order to restrict variations in the liquid composition. These runs are

TJ-38, TJ-41, TJ-20, TJ-15, TJ-12, TJ-11, TJ-27, TJ-19 and TJ-1 for the TJ composition [1] and 500B-43, 500B-22, 500B-30 and 500B-44 for the 500B composition [2]. In the 1 atm experiments, fO_2 was maintained at MW in TJ-27, at NNO in TJ-38 and at FMQ-1 in 500B-48 whereas in the high pressure experiments, fO_2 was estimated to lie between FMQ-4 and FMQ-2, the latter value being close to the CCO buffer [1]. Experiments were run under dry conditions as these are appropriate for anorthosite petrogenesis [18]. An additional crystallization experiment (TJ-15) was spiked with 1% Cr_2O_3. This experiment was held for 6 h above the liquidus at $T = 1200$°C in order to achieve complete homogenization of the charge. Then, the temperature was decreased to the liquidus ($T = 1160$°C) and held at this temperature for 64 h. Compositions of the experimental products of TJ-15 measured with the electron microprobe are given in Table 2.

The Cr concentrations were measured only in orthopyroxene–liquid pairs produced in the TJ experiments with the Cameca SX50 electron microprobe of the Lamont–Doherty Earth Observatory. Sr was measured in the plagioclase–liquid pairs produced in the experiments on both compositions with the Cameca SX100 electron microprobe at the American Museum of Natural History. For Sr determinations in plagioclase and glass, the accelerating voltage was set at 15 kV and SrLα, focussed through a LPET crystal, was measured for 360 s at a beam current of 30 nA for TJ experiments and for 300 s at a beam current of 50 nA for 500B experiments. A strontianite served as the Sr standard. Background positions were located from peak-free regions of wavelength scans on both sides of the SrLα peak; count times were half the peak time for each position and the average count rate of the two measurements was taken as the background. Peak count rates varied from 12 to 25 counts/s for the feldspars and glasses; backgrounds were typically ~9 counts/s. Results are shown in Tables 3 and 4. Several standard glasses (JDF, NIST SRM 610 and Corning glass-X) were used as controls. NIST SRM 610 has Sr concentrations measured by ICP-MS that range from 512 to 515 ppm [19]; our 10 microprobe analyses yielded 510 ± 80 ppm. The bulk compositions of TJ and 500B calculated from the experimental phase compositions by mass balance range from 560 to 606 ppm with a mean value at 585 ppm for TJ and from 518 to 551 ppm with a mean value at 536 ppm for 500B. These results are in good agreement with the bulk Sr content of the starting materials (TJ: 530 ppm [16]; 500B: 495 ppm [20]). For measurements of Cr in orthopyroxene and glass, the accelerating voltage was set at 20 kV and the Cr Kα peak was measured with a beam current of 50 or 100 nA during 200 s for glass and 100 s for orthopyroxene. The Cr standard was synthetic uvarovite, LiF110 was the focussing crystal and backgrounds were the average of two off-peak measurements. For glass analyses, the beam was rastered over square areas of 10 μm. Results are listed in Table 4.

Table 2
Composition of experimental products in TJ-15 ($t = 69$ h, $P = 10$ kbar, $T = 1160$°C)

Phase	n[a]	SiO_2	TiO_2	Al_2O_3	Cr_2O_3	FeO	MgO	MnO	CaO	K_2O	Na_2O	P_2O_5	Total	An/En/Fo
gl	5	49.54	4.76	14.64	0.07	13.75	3.98	0.15	6.91	1.11	3.44	1.52	99.88	
		0.41	0.41	0.26	0.02	0.52	0.13	0.02	0.24	0.08	0.08	0.21		
pl	5	58.16	0.14	26.56	0.00	0.34	0.06	0.00	8.57	0.50	6.17	0.00	100.50	42.13
		0.24	0.01	0.31	0.00	0.07	0.01	0.00	0.20	0.04	0.13	0.00		
opx	5	50.13	1.07	5.94	0.95	19.68	21.03	0.23	2.35	0.00	0.21	0.00	101.60	62.29
		0.29	0.23	0.73	0.09	0.62	0.92	0.01	0.59	0.00	0.11	0.00		
pig	7	49.94	1.27	5.54	1.00	17.59	18.06	0.25	7.07	0.00	0.50	0.00	101.23	54.71
		0.80	0.24	0.70	0.11	0.75	1.34	0.03	1.49	0.00	0.08	0.00		
crmt	1	0.13	10.94	18.33	26.98	38.27	6.29	0	0.17	0	0.02	0	101.13	

[a]Number of analyses performed on each phase. For each phase, the second row corresponds to the standard deviation; Fo, An, En are given in atomic units for olivine, plagioclase and pyroxene. Abbreviations: gl, glass; pl, plagioclase; opx, orthopyroxene; pig, pigeonite; crmt, chromite.

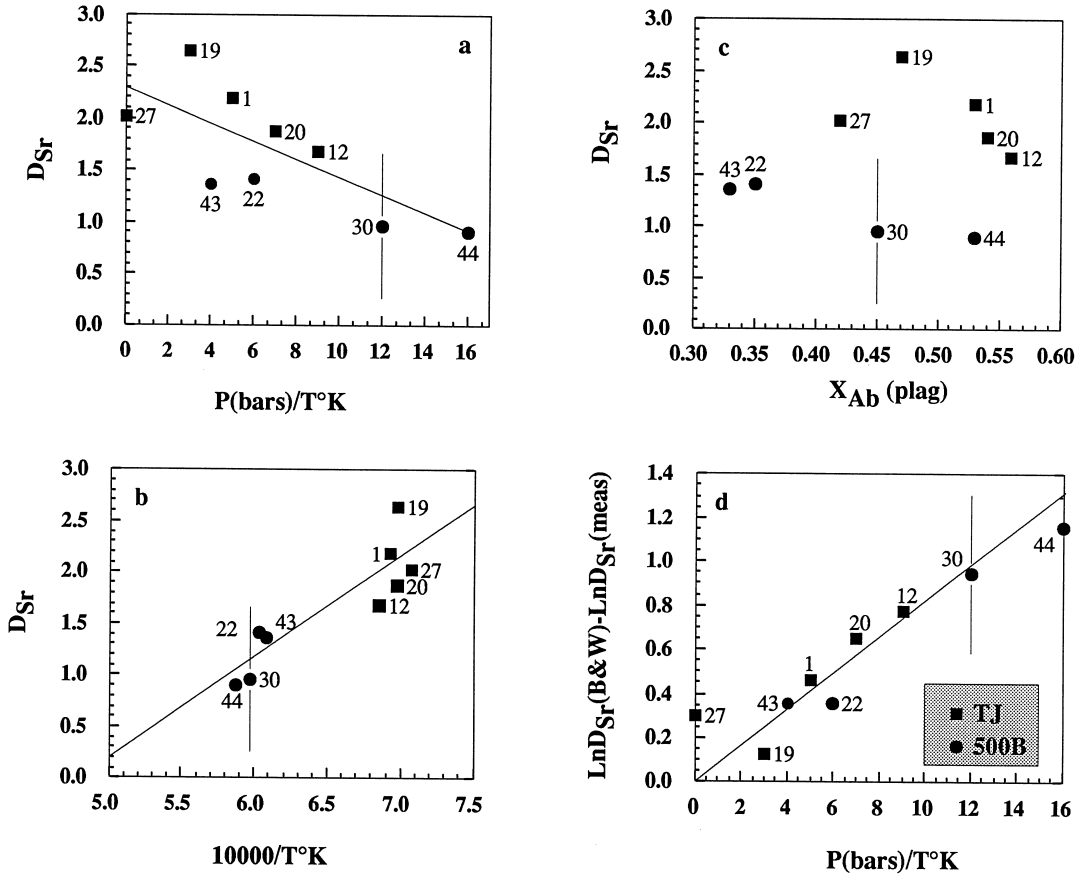

Fig. 1. Variation of D_{Sr} with pressure, temperature and plagioclase composition. Squares: TJ bulk composition; circles: 500B bulk composition. Error bars taken from standard deviation of 10 analyses of NIST SRM610 glass (see text). (a) D_{Sr} versus P (bars)/T (K). (b) D_{Sr} versus 10 000/T (K). (c) D_{Sr} versus X_{Ab} in plagioclase. (d) Deviation of D_{Sr} calculated by the method of Blundy and Wood [4] from measured values versus P/T ($R^2 = 0.83$).

3. Results and discussion

3.1. D_{Sr} (plag/melt)

Pressure, temperature, composition, crystal chemistry and liquid structure may all affect D_{Sr} between plagioclase and liquid. In our experiments, the liquid composition is nearly constant for runs conducted with the same starting composition because only liquidus or near liquidus experiments have been selected. Examination of Table 3 shows that the plagioclases in the TJ experiments are generally more heterogeneous than those in the 500B experiments and this heterogeneity leads to greater variation in the D_{Sr} values. We attribute the greater heterogeneity in the TJ plagioclases to the lower run temperatures. Indeed, the most heterogeneous plagioclase is in the lowest temperature run (TJ-27, 1140°C). As shown in Fig. 1a (see also Table 3), TJ-27 falls

→

Numbers in brackets represent the error on the partition coefficient (one standard deviation) which has been calculated with the following expression: $\sigma D_{Sr} = D_{Sr}((\sigma Sr \text{ in plag/Sr in plag})^2+(\sigma Sr \text{ in glass/Sr in glass})^2)^{1/2}$.

X_{An} (Ca/(Ca+Na+K) in atomic units) is the plagioclase composition. Abbreviations: gl, glass; pl, plagioclase.

[a]Number of analyses performed on each phase, the second row corresponds to the standard deviation.

Table 3
Partition coefficients of Sr between plagioclase and melt

Run	T (°C)	P	Phase	n[a]	SiO_2	TiO_2	Al_2O_3	Cr_2O_3	FeO	MgO	MnO	CaO	K_2O	Na_2O	P_2O_5	Sr (ppm)	Total	X_{An}	D_{Sr}
500B-43	1370	7 kbar	gl	3	54.69	0.55	22.80		3.29	1.38		9.29	0.89	4.66	0.13	516	97.73		
					0.13	0.01	0.08		0.03	0.02		0.07	0.02	0.03	0.11	34			
			pl	5	51.93	0.05	30.54		0.17	0.05		13.08	0.15	3.57		702	99.62	0.66	1.4 (0.2)
					0.41	0.02	0.17		0.02	0.00		0.17	0.02	0.10		17			
500B-22	1385	10 kbar	gl	3	55.01	0.48	22.49		3.27	1.45		9.31	0.94	4.62	0.19	516	97.81		
					0.31	0.02	0.16		0.12	0.01		0.14	0.01	0.07	0.16	17			
			pl	4	51.82	0.04	29.71		0.15	0.05		12.60	0.18	3.74		727	98.36	0.64	1.4 (0.2)
					0.30	0.01	0.19		0.03	0.00		0.22	0.01	0.12		101			
500B-30	1400	20 kbar	gl	3	54.83	0.67	22.11		3.53	1.49		9.19	0.96	4.47	0.06	575	97.38		
					0.35	0.02	0.04		0.07	0.01		0.08	0.01	0.07	0.05	25			
			pl	5	55.38	0.03	28.17		0.17	0.05		10.49	0.30	4.83		550	99.50	0.54	1.0 (0.1)
					0.55	0.02	0.28		0.03	0.01		0.41	0.01	0.16		51			
500B-44	1430	27 kbar	gl	3	56.32	0.65	21.18		3.70	1.13		8.68	1.08	4.64	0.11	609	97.56		
					0.11	0.02	0.16		0.09	0.02		0.04	0.01	0.12	0.06	25			
			pl	5	57.66	0.02	26.89		0.15	0.03		8.76	0.41	5.83		550	99.81	0.44	0.9 (0.1)
					0.23	0.01	0.12		0.03	0.01		0.05	0.01	0.05		34			
TJ-27	1140	1 atm	gl	5	50.20	4.30	15.62	0.01	13.31	4.51	0.16	6.54	1.03	3.64	0.62	533	100.00		
					0.35	0.13	0.10	0.00	0.08	0.08	0.01	0.09	0.02	0.06	0.02	42			
			pl	4	54.17	0.14	29.02		0.73	0.08		11.31	0.24	4.70		1074	100.51	0.56	2.0 (0.4)
					2.55	0.09	1.35		0.26	0.05		1.76	0.09	0.82		169			
TJ-19	1160	5 kbar	gl	5	48.67	4.73	14.65	0.01	14.42	5.05	0.15	6.27	1.20	3.64	0.62	465	99.46		
					0.48	0.18	0.58	0.01	0.55	0.22	0.03	0.07	0.03	0.12	0.06	25			
			pl	5	55.24	0.22	28.11		0.52	0.09		10.39	0.29	5.21		1226	100.20	0.52	2.6 (0.2)
					0.69	0.02	0.47		0.06	0.01		0.46	0.02	0.24		79			
TJ-1	1170	7 kbar	gl	5	49.25	4.28	15.55	0.01	13.25	4.51	0.15	6.59	1.03	3.76	0.62	567	99.06		
					0.35	0.18	0.10	0.00	0.20	0.07	0.03	0.08	0.03	0.03	0.06	42			
			pl	5	57.37	0.18	27.38		0.44	0.07		8.99	0.39	5.90		1235	100.87	0.45	2.2 (0.2)
					1.42	0.02	0.87		0.07	0.01		0.95	0.07	0.40		93			
TJ-20	1160	10 kbar	gl	5	48.84	4.53	15.40		13.12	4.11	0.13	6.66	1.03	3.56	0.64	592	98.11		
					0.14	0.09	0.09		0.20	0.10	0.02	0.04	0.02	0.06	0.05	42			
			pl	6	57.64	0.16	27.20		0.51	0.07		8.78	0.41	6.03	0.01	1109	100.94	0.44	1.9 (0.2)
					0.40	0.02	0.13		0.06	0.01		0.17	0.01	0.11	0.01	76			
TJ-12	1185	13 kbar	gl	5	48.77	4.28	15.91		12.50	4.11	0.13	6.73	0.96	3.60	0.60	600	97.66		
					0.16	0.04	0.08		0.13	0.07	0.03	0.03	0.01	0.05	0.03	59			
			pl	5	57.88	0.09	27.16		0.42	0.06		8.36	0.40	6.15		1006	100.63	0.42	1.7 (0.2)
					1.10	0.05	0.72		0.11	0.01		0.69	0.04	0.41		101			

Table 4
Partition coefficients of Cr between orthopyroxene and melt

Run#	fO_2	P	T (°C)	Opx (En)	Products	Cr in Opx	Cr in melt	D_{Cr}	D_{Cr} [7]
TJ-38	NNO	1 atm	1133	0.84	gl, pl, opx, il, mt	39	18	2 (1)	5.7
TJ-41	FMQ-2 to FMQ-4	7 kbar	1155	0.66	gl, pl, opx	313	39	8 (3)	4.2
TJ-20	FMQ-2 to FMQ-4	10 kbar	1160	0.65	gl, pl, opx	379	36	10 (3)	4.2
TJ-15	FMQ-2 to FMQ-4	10 kbar	1160	0.62	gl, pl, opx, pig, crmt	6348	447	14.2 (0.4)	4.2
TJ-12	FMQ-2 to FMQ-4	13 kbar	1185	0.67	gl, pl, opx	386	44	9 (4)	3.7
TJ-11	FMQ-2 to FMQ-4	13 kbar	1162	0.61	gl, pl, opx, pig, aug, il	231	22	11 (3)	4.1

Numbers in brackets represent the error on the partition coefficient expressed as one standard deviation and calculated with the following expression: $\sigma D_{Cr} = D_{Cr}\{(\sigma Cr \text{ in opx/Cr in opx})^2+(\sigma Cr \text{ in glass/Cr in glass})^2\}^{1/2}$.
Abbreviations: gl, glass; pl, plagioclase; opx, orthopyroxene; pig, pigeonite; aug, augite; il, ilmenite; mt, magnetite; crmt, chromite.

off a general trend of D_{Sr} decreasing with pressure displayed by the other TJ runs and separately by the 500B runs. The overall decrease is relatively small, however. Fig. 1b shows a very good correlation between D_{Sr} and inverse temperature. It is evident though that the temperature intervals covered by the runs for each bulk composition are relatively small (45°C for TJ and 75°C for 500B) and that D_{Sr} also differs significantly with composition between the two starting materials. So it is not immediately clear whether temperature or composition is the more important factor. Fig. 1c shows that there are small decreases in D_{Sr} with increasing Ab content in plagioclase for each bulk composition. However, there can also be very significant differences in D_{Sr} between plagioclases with a similar composition.

Several petrological studies ([21–23]; the data of [24] in [25,4]) have shown that D_{Sr} markedly increases with increasing albite in plagioclase. Based on a large dataset of experimental (plag/liq) and volcanic (phenocryst/matrix) compositions, Blundy and Wood [4] have argued that the correlation of D_{Sr} and albite content can be explained by the albite structure being more elastic than that of anorthite. These authors also inferred a small increase in D_{Sr} with decreasing temperature for comparable plagioclase compositions, but were not able to distinguish any correlation of D_{Sr} with either liquid composition or pressure. Accordingly, they derived a semi- empirical relationship relating D_{Sr} to X_{An} and T ($RT\ln D_{Sr} = -26\,700X_{An}+26\,800$). More recently, D_{Sr} has been reanalyzed in the experimental charges of Drake [26] and a semi-empirical relationship relating D_{Sr}, T and X_{An} ($RT\ln D_{Sr} = -30\,400X_{An}+28\,500$) very similar to that of Blundy and Wood has been proposed [5]. On the other hand, other authors [6,7,25] have emphasized the control of the liquid composition. The D_{Sr} derived from Drake's experiments [24] displays a direct correlation with the augite content of the liquid ($D_{Sr} = 1.4+0.023di_L$) [25]. Morse [6] also observed that in Kiglapait, D_{Sr} appears to correlate inversely with the amount of non-feldspathic components present in the liquid until 60% crystallization. In another model [7], the dependence of trace element partitioning on variations in liquid composition has been accommodated by the use of complex partition coefficients that incorporate terms for the activities of liquid components.

In our experiments, plagioclase becomes more albitic and less anorthitic with increasing pressure (TJ: An_{56} at 1 atm decreases to An_{42} at 13 kbar; 500B: An_{66} at 5 kbar decreases to An_{44} at 27 kbar [8]). Consequently, D_{Sr} should increase with increasing pressure if the albite content in plagioclase is the dominant control. For example, given the overall variation of plagioclase experiments (An_{66}–An_{42}), the semi-empirical expression of Blundy and Wood and the modelling of Sr abundances in the BKSK intrusion [23] both predict an increase of approximately 1.0 in the D_{Sr}. Such large increases are not observed in the experiments and, in fact, D_{Sr} decreases slightly with in-

creasing Ab for each composition. Therefore, we suggest that the unexpected behavior of D_{Sr} is due to the combined effects of increasing pressure and temperature neutralizing the effects of plagioclase crystal chemistry. The ionic radius of Sr^{2+} (1.18 [27]) is significantly higher than those of Ca^{2+} (1.00) and Na^{+} (1.02) (Ca, Na and Sr all enter the eight-fold coordinated M-site in plagioclase [5]). The partial molar volume of $SrAl_2Si_2O_8$ is thus higher than that of $CaAl_2Si_2O_8$ and $NaAlSi_3O_8$ and increasing pressure decreases the ability of $SrAl_2Si_2O_8$ to substitute for $CaAl_2Si_2O_8$ and $NaAlSi_3O_8$. A similar decrease of pressure in D_{Ba} between alkali feldspar and silicate liquid has also been reported by Guo and Green [28].

We have calculated D_{Sr} using the Blundy and Wood algorithm for the temperatures and plagioclase compositions of the runs listed in Table 3 and have plotted the difference between the natural logarithms of the calculated and measured Ds versus P/T in Fig. 1d (see also Table 5). Fig. 1d shows that the Blundy and Wood model overestimates every measured D_{Sr} and that the overestimates increase with P/T. The increasing deviation between predicted and measured D_{Sr} with pressure is consistent with the inference made above that D_{Sr} (i.e. the solubility of $SrAl_2Si_2O_8$) decreases with increasing pressure.

Table 5 displays a comparison between D_{Sr} measured at 1 atm and D_{Sr} calculated with the above mentioned models. The predictions of the Bindeman et al. [5] model are very similar to those of the Blundy and Wood model and consistently overestimate our measured values of D_{Sr}; whereas the Nielsen [7] and Morse [6] models typically underestimate D_{Sr}. Although these discrepancies are not especially severe with respect to analytical uncertainty, nevertheless, when precise modelling is needed at mid to lower crustal processes, a correction for pressure is obviously important. For example, in the modelling of the jotunite liquid line of descent [17,23], the first stage of differentiation at mid to lower crustal pressure drives the liquid from a primitive jotunite (like TJ) to an evolved jotunite by subtraction of a cumulate dominated by plagioclase (74% plagioclase+16% orthopyroxene+10% ilmenite). Using the range of D_{Sr} measured in TJ-19 and -20 (2.6–1.9), the Sr content in the evolved jotunite ranges from 279 to 400 ppm compared with 227 to 167 ppm obtained with the respective D_{Sr} from Blundy and Wood and 668 to 517 ppm obtained with the respective D_{Sr} from Nielsen [7]; whereas the Sr content of the fine-grained evolved jotunites from the Rogaland Province ranges from 354 up to 465 ppm with a mean value of 429 ppm. Thus the Sr concentrations calculated with the measured D_{Sr} overlap with the range of observed values, whereas results calculated with modelled D_{Sr} are out of this range. Consequently, even though semi-empirical models predict values of D_{Sr} reasonably well at low pressures, the addition of pressure terms are obviously needed to model high-pressure processes accurately. As a preliminary step we offer the following simple adjustment to the Blundy and Wood model based on the correlation in Fig. 1d:

$$\ln D_{Sr}(P,\ T,\ X) = \ln D_{Sr}(\mathrm{BW}) - 0.00821P\ (\mathrm{bar})/T\ (\mathrm{K})$$

Table 5
Comparison between measured and calculated D_{Sr}

	P (kbar)	T (K)	X_{An}	D_{Sr}, this study	D_{Sr} [4]	D_{Sr} [5]	D_{Sr} [7]	D_{Sr} [6]
TJ-27	0.001	1413	0.56	2.0	2.7	2.6	1.5	1.7
TJ-19	5	1433	0.52	2.6	3.0	2.9	0.9	1.7
TJ-1	7	1443	0.45	2.2	3.5	3.5	1.4	1.7
TJ-20	10	1433	0.44	1.9	3.6	3.6	1.4	1.7
TJ-12	13	1458	0.42	1.7	3.6	3.7	1.4	1.6
500B-43	7	1643	0.66	1.4	1.9	1.8	1.3	1.2
500B-22	10	1658	0.64	1.4	2.0	1.9	1.2	1.2
500B-30	20	1673	0.54	1.0	2.5	2.4	1.1	1.2
500B-44	27	1703	0.44	0.9	2.9	2.9	0.9	1.2

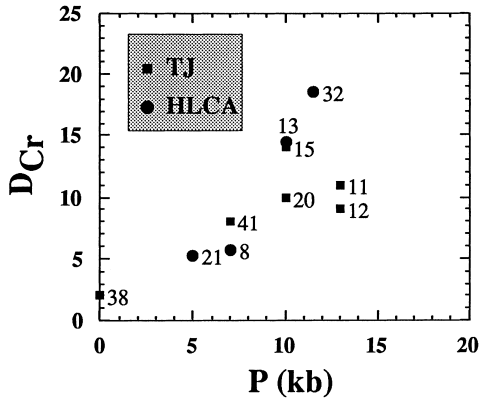

Fig. 2. Measured D_{Cr} versus pressure in two experimental datasets (TJ: [1]; HLCA: [2]).

3.2. D_{cr} (opx/melt)

Here again, considering the small ranges of temperature and compositions of liquids in the selected experiments, the only variables which can possibly affect D_{Cr} are fO_2 and pressure. Cr is present as Cr^{3+} and Cr^{2+}. D_{Cr} (opx/melt) increases with oxygen fugacity and an empirical expression relating the Cr oxidation ratio to temperature and oxygen fugacity ($\log(Cr^{3+}/Cr^{2+})liq = -4.50+(10\,900/T)+0.25 \log fO_2$) was derived from an experimental dataset [29]. The increase of D_{Cr} with fO_2 indicates that Cr^{3+}, which has the smaller ionic radius (0.615 Å versus 0.80 Å for Cr^{2+} [27]) substitutes more readily into the orthopyroxene structure than Cr^{2+}. In our experiments, the oxygen fugacity was controlled at NNO by mixing CO and CO_2 gases for TJ-38 (1 atm); whereas in charges run at higher pressures in graphite capsules a combination of crystallization sequences and the compositions of oxide phases suggest oxygen fugacities between FMQ-4 and FMQ-2 [1]. Consequently, the D_{Cr} obtained at 1 atm is significantly higher than what would have been obtained at the more reducing conditions of the high pressure experiments.

The measured values of D_{Cr} from the TJ experiments increase with pressure as illustrated in Fig. 2. Even though the precision of the analyses of the D_{Cr} obtained in experiments with natural Cr abundances is relatively poor, the D_{Cr} determined from the doped run (TJ-15) lies squarely on the trend formed by the lower precision analyses. Ds calculated with data from melting experiments on a high-Al basalt composition (HLCA) [2] show similar increases with pressure. D_{Cr} is also strongly correlated with $D_{Al_2O_3}$ (Fig. 3), which increases with pressure [8] as well. Although Cr^{3+} substitution in orthopyroxene in the form of a $MgCrAlSiO_6$ component is likely to be enhanced by the presence of Al^{3+} for charge balancing, Cr is nevertheless present as a trace element whereas the Al_2O_3 content ranges from 1.58 to 7.99% in the TJ and HLCA orthopyroxenes. Consequently, even at low pressure Al in orthopyroxenes crystallized from plagioclase-saturated liquids will always be well in excess of the Cr present. Thus the Cr^{3+} is saturated with Al^{3+} and, therefore, increasing the Al^{3+} has little effect on Cr partitioning. Accordingly, we suggest that D_{Cr} and $D_{Al_2O_3}$ are positively correlated because they both increase with pressure. Here too, the smaller ionic radius of Cr^{3+} (0.615 Å) relative to those of Mg^{2+} (0.72 Å) and Fe^{2+} (0.78 Å) is probably responsible of the enhanced solubility of Cr with pressure.

The D_{Cr} calculated with the model of Nielsen [7] for the 1 atm experiment (TJ-38) is higher (5.7) than the measured value (2) (Table 4). Here, too, partitioning models need to be modified so as to accommodate pressure effects.

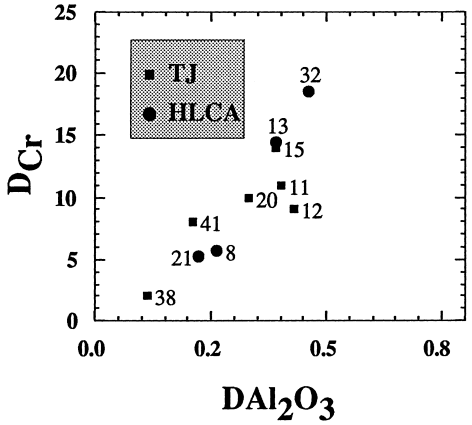

Fig. 3. D_{Cr} versus $D_{Al_2O_3}$ in two experimental datasets (TJ: [1]; HLCA: [2]).

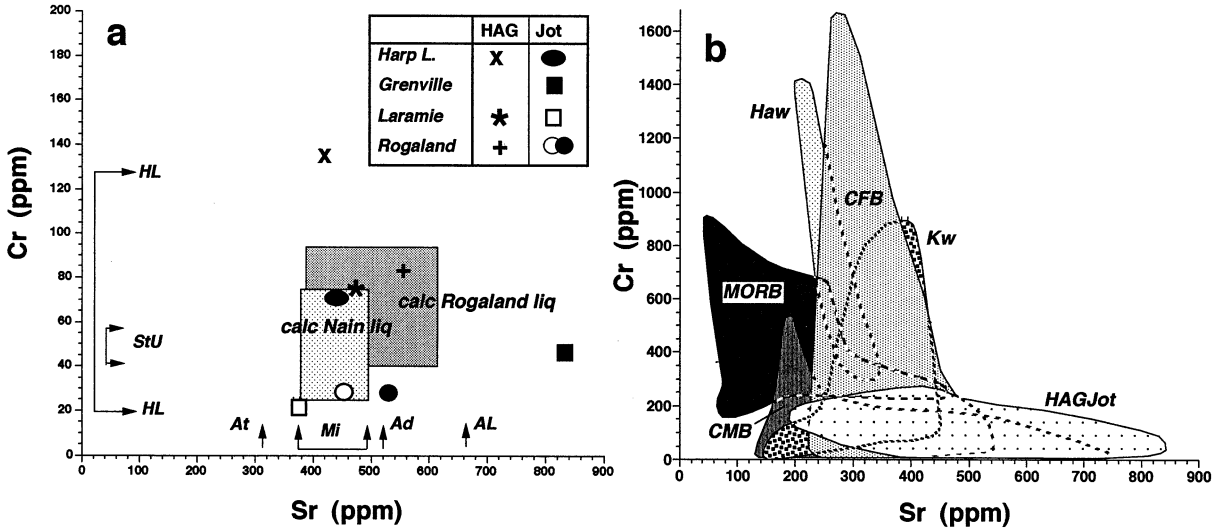

Fig. 4. Sr and Cr concentrations in parental magmas. (a) Comparison of high-Al gabbro (HAG) and primitive jotunite (Jot) compositions with concentrations of Sr and Cr calculated from megacryst compositions and $D_{Sr} = 1.8$ and $D_{Cr} = 14$. Sources for Sr: Harp Lake HAG average of 16 analyses [41], Jot (EC90-216, [42]); Grenville Jot (sample 738, [33]); Laramie HAG average of 43 analyses [43], Jot (BM-14, [37]); Rogaland HAG average of 10 analyses [44], Jot (TJ, [16]). Sources for Cr: Harp Lake HAG average of 16 analyses [41], Jot (EC90-216, [42]); Grenville Jot (sample 738, [33]); Laramie HAG average of 41 analyses [43], Jot (BM-14, [37]); Rogaland HAG average of nine analyses [44], Jot (TJ, [16]). Boxes indicate calculated compositional ranges where data is available for both opx(Cr) and plag(Sr) megacrysts: Nain [45], Rogaland [46]. Arrows indicate calculated liquid compositions where data is available for only one type of megacryst: Cr (opx): HL (Harp Lake, [41]) and StU (St. Urbain, [35]), and Sr (plag): AL, At, Ad (Allard Lake, Atikonak, and Adirondack, respectively, [47]) and Mi (Michikamau, [11]). (b) Comparison of Sr and Cr concentrations in members of the HAG/Jot suite with Sr and Cr concentrations in common basalts. Additional data for HAG/Jot from [43] and [36]; MORB [48–50]; convergent margin basalts, CMB [51,52]; Keweenawan lavas, Kw [52]; continental flood basalts, CFB [52,53]; Hawaiian tholeiites, Haw [52].

4. Implications for anorthosite petrogenesis

The data presented here on D_{Cr} and D_{Sr} at lower crustal pressures enable us to estimate the Sr and Cr contents of magmas parent to massive anorthosites by using known compositions of plagioclase and orthopyroxene megacrysts. It has been shown that these orthopyroxene and plagioclase megacrysts, so characteristic of massif-type anorthosites [9–12], are liquidus phases which have crystallized at lower crustal pressures from the parent magmas of the anorthosites and were then rafted within the anorthosite diapir rising up to upper crustal pressures. Liquid compositions calculated to be in equilibrium with these megacrysts ought to thus be those of the deep-seated anorthosite parent magmas. We thus have used values of D_{Sr} (1.8, plag) and D_{Cr} (14, opx) appropriate to 10 kbar. On the basis of redox effects discussed above, D_{Cr} probably represents a minimum value for anorthosites parent magmas, which probably crystallized at a fO_2 close to FMQ. Results of these calculations are presented in Fig. 4a.

Possible parent magmas of massive anorthosites encompass a large continuum of compositions [30] ranging from high-Al gabbros like HLCA to primitive jotunites like TJ, with high-Al basalts being parent to labradorite anorthosites [2] and primitive jotunites being parent to andesine anorthosites [17,31–32]. We have thus selected Cr and Sr data from the literature for primitive jotunites and high-Al gabbros whose petrologic evidence suggests are close to liquid compositions. Fig. 4a shows that the calculated Sr and Cr concentrations of the megacryst parental liquids are in the range of those observed in average primitive jotunites (Jot) and high-Al gabbros (HAG) from

several massifs, which is consistent with the hypothesis that primitive jotunites and high-Al gabbros are the parent magmas of massive anorthosites. In some massifs, e.g. Labrieville [33], there are no primitive jotunites, let alone gabbroic rocks. However, here too application of our Ds to megacryst plagioclase (2100 ppm [34]) and orthopyroxene (45–353 ppm [35]) yields calculated liquid compositions (3–25 ppm Cr, 1170 ppm Sr) that are quite similar to typical jotunites (2–8 ppm Cr, 660–1225 ppm Sr [33]).

The primitive HAG/Jot suite has a combination of high Sr (350–810 ppm) and low Cr (9–250 ppm) that is unusual, but not unique among basalts. In Fig. 4b we compare the range of Sr and Cr concentrations in individual (not average) analyses of HAG/Jot to those of other basalts. Primitive basalts from each suite typically have the highest Cr and lowest Sr; whereas more evolved basalts have lower Cr and higher Sr, a feature that is consistent with both fractionation and crustal contamination. Fig. 4b shows that the HAG/Jot suite overlaps with the evolved ends of the convergent margin basalt (CMB), continental flood basalt (CFB) and Keweenawan lava (Kw) suites, but apparently does not have a prominent high Cr trend. Remarkably, even relatively oxide-rich mafic rocks do not have high Cr concentrations [36–37]. However, despite similarities in Sr, Cr and even Mg# to evolved convergent margin and flood basalts, we have previously shown [30,38] that high-Al gabbros and primitive jotunites typical of Proterozoic massifs are distinct from other basaltic rocks in that they have lower wollastonite contents and project along the 10 to 13 kbar sections of the opx+cpx+plag liquidus boundary rather than along lines of descent that indicate pressures <4 kbar. Several of the HAG/Jot compositions also lie astride the thermal maximum on the opx+cpx+plag liquidus boundary, a feature that precludes their being derived at lower crustal pressures by fractional crystallization, with or without assimilation. Instead, these compositions require melting of mafic (pyroxene+plagioclase) sources. The data presented here require that these sources must be low in Cr and high in Sr. Estimates of the composition of the lower continental crust [39] satisfy both the major and trace element criteria.

5. Conclusions

1. The combined and opposing effects of crystal chemistry and pressure produce relatively minor change in D_{Sr} (plag/liquid) with increasing pressure. D_{Sr} decreases with pressure but increases with the albitic content of plagioclase, which itself increases with pressure.
2. This small decrease in D_{Sr} with pressure implies that the high Sr content of plagioclase megacrysts from massive anorthosites results from the high Sr content of their parent magmas and of the source rock of the latter.
3. There is a significant increase of D_{Cr} (opx/liquid) with pressure, which probably results from Cr^{3+} having a smaller ionic radius than Fe^{2+} and Mg^{2+}. Moreover, the increase of D_{Cr} accounts for the very high Cr concentrations observed in the orthopyroxene megacrysts from massive anorthosite complexes.
4. Sr and Cr concentrations calculated for the 10 kbar parental liquids of orthopyroxene and plagioclase megacrysts from several massifs are similar to those of high-Al gabbros and primitive jotunites (hypersthene monzodiorites) which are the likely parent magmas of massive anorthosites.

Acknowledgements

The authors gratefully thank Miranda Fram (US Geological Survey, Sacramento) for providing the 500B experimental charges. J.V.A. and J.C.D. were funded by the Belgian Fund for Joint Basic Research (FRFC) and J.L. by NASA grants NAGW-3407 and NAG5-4649. This work was also part of the International Geological Correlation Program, project 290 (Anorthosites and Related Rocks). This manuscript was improved by the critical and constructive reviews of J. Blundy, R. Nielsen and E. Cottrell. *[CL]*

References

[1] J. Vander Auwera, J. Longhi, Experimental study of a jotunite (hypersthene monzodiorite): constraints on the parent magma composition and crystallization conditions (P, T, fO_2) of the Bjerkreim–Sokndal layered intrusion (Norway), Contrib. Miner. Petrol. 118 (1994) 60–78.

[2] M. Fram, J. Longhi, Phase equilibria of dikes associated with Proterozoic anorthosites complexes, Am. Miner. 77 (1992) 605–616.

[3] R. Wiebe, Anorthositic magmas and the origin of Proterozoic anorthosite massifs, Nature 286 (1980) 564–567.

[4] J. Blundy, B. Wood, Crystal-chemical control on the partitioning of Sr and Ba between plagioclase feldspar, silicate melts and hydrothermal solutions, Geochim. Cosmochim. Acta 55 (1991) 193–209.

[5] I. Bindeman, A. Davis, M. Drake, Ion microprobe study of plagioclase–basalt partition experiments at natural concentration levels of trace elements, Geochim. Cosmochim. Acta 62 (1998) 1175–1193.

[6] S. Morse, Partitioning of strontium between plagioclase and melt: a comment, Geochim. Cosmochim. Acta 56 (1992) 1735–1738.

[7] R. Nielsen, BIGD.FOR: a fortran program to calculate trace-element partition coefficients for natural mafic and intermediate composition magmas, Comput. Geosci. 18 (1992) 773–788.

[8] J. Longhi, M. Fram, J. Vander Auwera, J. Montieth, Pressure effects, kinetics, and rheology of anorthositic and related magmas, Am. Miner. 78 (1993) 1016–1030.

[9] L.D. Ashwal, Anorthosites, Springer, Heidelberg, 1993.

[10] R. Emslie, Pyroxene megacrysts from anorthositic rocks: new clues to the sources and evolution of the parent magmas, Can. Miner. 13 (1975) 138–145.

[11] R. Emslie, Proterozoic Anorthosite massifs, in: A.T. Tobi, J.L.R. Touret (Eds.), The Deep Proterozoic Crust in the North Atlantic Provinces, Ser. C158, Nato Advanced Study Institute, Reidel, 1985, pp. 39–60.

[12] R. Maquil, J. Duchesne, Géothermométrie par les pyroxènes et mise en place du massif anorthositique d'Egersund-Ogna (Rogaland, Norvège méridionale), Ann. Soc. Géol. Belg. 107 (1984) 27–49.

[13] J. Berg, Dry granulite mineral assemblages in the contact aureole of the Nain Complex, Labrador, Contrib. Miner. Petrol. 64 (1977) 32–52.

[14] B. Jansen, A. Blok, M. Scheelings, Geothermometry and geobarometry in Rogaland and preliminary results from the Bamble area, south Norway, in: A. Tobi, J.L.R. Touret (Eds.), The Deep Proterozoic Crust in the North Atlantic Provinces, Ser. C158, NATO Advanced Science Institute, Reidel, Dordrecht, 1985, pp. 499–518.

[15] J. Valley, J. O'Neil, Oxygen isotope evidence for shallow emplacement of Adirondack anorthosite, Nature 300 (1978) 497–500.

[16] J.C. Duchesne, J. Hertogen, Le magma parental du lopolithe de Bjerkreim-Sokndal (Norvège méridionale), C. R. Acad. Sci. Paris 306 (2) (1988) 45–48.

[17] J. Vander Auwera, J. Longhi, J.C. Duchesne, A liquid line of descent of the jotunite (hypersthene monzodiorite) suite, J. Petrol. 39 (1998) 439–468.

[18] S.A. Morse, A partisan review of Proterozoic Anorthosites, Am. Miner. 65 (1982) 1087–1100.

[19] N. Pearce, W. Perkins, J. Westgate, M. Gorton, S. Jackson, C. Neal, S. Chenery, A compilation of new and published major and trace element data for NIST SRM 610 and NIST SRM 612 glass reference materials, Geostand. Newsl. 21 (1997) 115–144.

[20] R. Wiebe, Evidence for unusually feldspathic liquids in the Nain Complex, Labrador, Am. Miner. 75 (1990) 1–12.

[21] M. Korringa, D. Noble, Distribution of Sr and Ba between natural feldspar and igneous melt, Earth Planet. Sci. Lett. 11 (1971) 147–151.

[22] B. Jensen, Patterns of trace element partitioning, Geochim. Cosmochim. Acta 37 (1973) 2227–2242.

[23] J.C. Duchesne, Quantitative modeling of Sr, Ca, Rb and K in the Bjerkrem-Sogndal lopolith (SW Norway), Contrib. Miner. Petrol. 66 (1978) 175–184.

[24] M.J. Drake, The Distribution of Major and Trace Elements between Plagioclase Feldspar and Magmatic Liquid: an Experimental Study, Ph.D. thesis, University of Oregon, 1972.

[25] S. Morse, Kiglapait geochemistry V: strontium, Geochim. Cosmochim. Acta 46 (1982) 223–234.

[26] M.J. Drake, D. Weill, Partition of Sr, Ba, Eu^{2+}, Eu^{3+}, and other REE between plagioclase feldspar and magmatic liquid: an experimental study, Geochim. Cosmochim. Acta 39 (1975) 689–712.

[27] R. Shannon, Revised effective ionic radii and systematic studies of interatomic distances in halides and chalcogenides, Acta Cryst. 32 (1976) 751–767.

[28] J. Guo, T. Green, Barium partitioning between alkali feldspar and silicate liquid at high temperature and pressure, Contrib. Miner. Petrol. 102 (1989) 328–335.

[29] S. Barnes, The distribution of chromium among orthopyroxene, spinel and silicate liquid at atmospheric pressure, Geochim. Cosmochim. Acta 50 (1986) 1889–1909.

[30] J. Longhi, J. Vander Auwera, Polybaric fractionation and the connection between high-Al gabbro and monzonorite, IGCP 290, Origin of Anorthosites and Related Rocks, Moi, Norway, 1992.

[31] J.C. Duchesne, D. Demaiffe, Trace elements and anorthosite genesis, Earth Planet. Sci. Lett. 38 (1978) 249–272.

[32] D. Demaiffe, J. Hertogen, Rare earth geochemistry and strontium isotopic composition of a massif-type anorthositic–charnockitic body: the Hidra massif (Rogaland, SW Norway), Geochim. Cosmochim. Acta 45 (1981) 1545–1561.

[33] B.E. Owens, M.W. Rockow, R.F. Dymek, Jotunites from the Grenville Province. Quebec petrological characteristics and implications for massif anorthosite petrogenesis, Lithos 30 (1993) 57–80.

[34] B. Owens, R. Dymek, R. Tucker, J. Brannon, F. Podosek, Age and radiogenic isotopic composition of a late- to

post-tectonic anorthosite in the Grenville Province Labrieville massif, Quebec, Lithos 31 (1994) 189–206.
[35] B. Owens, R. Dymek, Significance of pyroxene megacrysts for massif anorthosite petrogenesis: constraints from the Labrieville, Quebec, pluton, Am. Miner. 80 (1995) 144–161.
[36] K. Olsen, Rocks in the anorthosite-bearing Adirondack Highlands, J. Petrol. 33 (1992) 471–502.
[37] J. Mitchell, J. Scoates, C. Frost, A. Kolker, The geochemical evolution of anorthosite residualmagmas in the Laramie anorthosite complex, Wyoming, J. Petrol. 37 (1996) 637–660.
[38] J. Longhi, J. Vander Auwera, M. Fram, J.C. Duchesne, Some phase equilibrium constraints on the origin of Proterozoic massif anorthosites and related rocks, J. Petrol. (1998).
[39] R. Rudnick, D. Fountain, Nature and composition of the continenetal crust a lower crustal perspective, Rev. Geophys. 33 (1995) 267–309.
[40] V. Kress, I. Carmichael, The compressibility of silicate liquids containing Fe_2O_3 and the effect of composition, temperature, oxygen fugacity and pressure on their redox states, Contrib. Miner. Petrol. 108 (1991) 82–92.
[41] R. Emslie, Geology and petrology of the Harp Lake Complex, central Labrador: an example of Elsonian magmatism, Geol. Surv. Can. Bull. 293 (1980) 136.
[42] R.F. Emslie, M.A. Hamilton, R.J. Thériault, Petrogenesis of a mid-Proterozoic anorthosite–mangerite–charnockite–granite (AMCG) complex: isotopic and chemical evidence from the Nain Plutonic Suite, J. Geol. 102 (1994) 539–558.
[43] J. Mitchell, J. Scoates, C. Frost, High-Al gabbros in the Laramie Anorthosite Complex, Wyoming: implications for the composition of melts parental to Proterozoic anorthosite, Contrib. Miner. Petrol. 119 (1995) 166–180.
[44] D. Demaiffe, B. Bingen, P. Wertz, J. Hertogen, Geochemistry of the Lyngdal hyperites (SW Norway) comparison with the monzonorites associated with the Rogaland anorthosite complex, Lithos 24 (1990) 237–250.
[45] S. Xue, S. Morse, Chemical characteristics of plagioclase and pyroxene megacrysts and their significance to the petrogenesis of the Nain anorthosites, Geochim. Cosmochim. Acta 58 (1994) 4317–4331.
[46] J.C. Duchesne, R. Maquil, The Egersund-Ogna massif, in: C. Maijer, P. Padget (Ed.), The Geology of southernmost Norway: an Excursion Guide, Norges Unders, Special Publication 1, 1987, pp. 50–56.
[47] R. Emslie, E. Hegner, Reconnaissance isotope geochemistry of anorthosite–mangerite–charnockite–granite (AMCG) complexes, Grenville Province, Canada, Chem. Geol. 106 (1993) 279–298.
[48] R. Batiza, Y. Niu, Petrology and magma chamber processes at the East Pacific Rise 9°30′N, J. Geophys. Res. 97 (1992) 6779–6797.
[49] F. Frey, W. Bryan, G. Thompson, Atlantic ocean floor: geochemistry and petrology of basalts from legs 2 and 3 of the Deep-Sea Drilling Project, J. Geophys. Res. 79 (1974) 5507–5527.
[50] S. Sun, R. Nesbitt, A. Shraskin, Geochemical characteristics of mid-ocean ridge basalts, Earth Planet. Sci. Lett. 44 (1979) 119–138.
[51] L. Lopez-Escobar, F. Frey, M. Vergara, Andesites and high-alumina basalts from central-south Chile high Andes: geochemical evidence bearing on their petrogenesis, Contrib. Miner. Petrol. 63 (1977) 199–228.
[52] B.V.S. Project, Basaltic Volcanism on the Terrestrial Planets, Pergamon, New York, 1981.
[53] P. Krishnamurthy, K. Cox, Picritic basalts and related lavas from the Deccan Traps of Western India, Contrib. Miner. Petrol. 62 (1977) 53–75.